HHS Public Access

Author manuscript

Mol Neurobiol. Author manuscript; available in PMC 2017 October 01.

Published in final edited form as:

Mol Neurobiol. 2016 October ; 53(8): 5066–5078. doi:10.1007/s12035-015-9413-x.

Tissue Transglutaminase and Its Product Isopeptide Are Increased in Alzheimer's Disease and APPswe/PS1dE9 Double Transgenic Mice Brains

Ji Zhang[1], **Suqing Wang**[2], **Wei Huang**[4], **David A. Bennett**[3], **Dennis W. Dickson**[5], **Dengshun Wang**[4], and **Rui Wang**[1]

[1] Shanghai Key Laboratory of New Drug Design, School of Pharmacy, East China University of Science and Technology, 130 Meilong Road, Shanghai 200237, China

[2] Department of Nutrition and Food Health, School of Public Health, Wuhan University, Wuhan, China

[3] Rush Alzheimer's Disease Center, Rush University Medical Center, Chicago, IL, USA

[4] Department of Pathology and Laboratory Medicine, School of Medicine and Public Health, University of Wisconsin, 1300 University Avenue, Madison, WI 53706, USA

[5] Department of Pathology (Neuropathology) and Neuroscience, Mayo Clinic College of Medicine, Jacksonville, FL 32224, USA

Abstract

Alzheimer's disease (AD) is characterized by intracellular and extracellular protein aggregates, including microtubule-associated protein tau and cleavage product of amyloid precursor protein, β-amyloid (Aβ). Tissue transglutaminase (tTG) is a calcium-dependent enzyme that cross-links proteins forming a γ-glutamyl-ε-lysine isopeptide bond. Highly resistant to proteolysis, this bond can induce protein aggregation and deposition. We set out to determine if tTG may play a role in pathogenesis of AD. Previous studies have shown that tTG and isopeptide are increased in advanced AD, but they have not addressed if this is an early or late feature of AD. In the present study, we measured tTG expression levels and enzyme activity in the brains of individuals with no cognitive impairment (NCI), mild cognitive impairment (MCI), and AD, as well as a transgenic mouse model of AD. We found that both enzyme expression and activity were increased in MCI as well as AD compared to NCI. In the transgenic model of AD, tTG expression and enzyme activity increased sharply with age and were relatively specific for the hippocampus. We also assessed overlap of isopeptide immunoreactivity with neurodegeneration-related proteins with Western blots and found neurofilament, tau, and Aβ showed co-localization with isopeptide in both AD and transgenic mice. These results suggest that tTG might be a key factor in pathogenesis of abnormal protein aggregation in AD.

Dengshun Wang dwang6@wisc.edu, Rui Wang ruiwang@ecust.edu.cn.

Conflict of Interest The authors declare that they have no competing interests.

Keywords

Alzheimer's disease (AD); Tissue transglutaminase (tTG); Cross-link; Isopeptide; γ-Glutamyl-ε-lysine; Aggregate

Introduction

Alzheimer's disease (AD) is a devastating neurodegenerative disease characterized by progressive cognitive impairment culminating in dementia. Senile plaques (SPs), neurofibrillary tangles (NFTs), and cerebral amyloid angiopathy (CAA) are the major pathologic features of AD [1–3]. Both SPs and CAA consist of extracellular deposits of β-amyloid protein (Aβ), with molecular weight of 4 kDa [4, 5]. Aβ oligomer aggregates or associated cellular reactions to the aggregates are thought to be neurotoxic [6, 7]. In CAA, Aβ accumulates in the outer portion of the media of blood vessels, which leads to degeneration of vascular smooth muscle cells [8, 9]. NFTs detected in the cytoplasm of neurons as paired helical filaments are composed of hyperphosphorylated tau protein [10]. One of possible toxic effects of Aβ is stimulation of tau hyperphosphorylation and aggregation through increases in intracellular calcium levels [11]. Biomarker studies suggest that accumulation of toxic Aβ species precedes the formation of hyperphosphorylated tau in NFTs in the neocortex [12].

Tissue transglutaminase (tTG), which is also called transglutaminase-2 (TG2), a monomeric protein with a molecular weight of 77–85 kDa, belongs to the family of transglutaminases (EC 2.3.2.13). The transglutaminase family consists of nine members—factor XIII-A subunit, TG1, tTG (TG2), TG3, TG4 through TG7, and Band 4.2 [13]. The first five ones are enzymatically active in humans. Transglutaminase proteins are ubiquitous in humans, but only TG1, tTG, and TG3 can be detected in human brains, especially in frontal cortex [14, 15]. Of the three, tTG has the highest expression in human brains. Evidence suggests that tTG can be expressed in both neurons and glial cells [14], and that it is expressed in cytosol, cell membranes, and extracellular fractions but also in the nucleus of neuroblastoma cells [16].

Tissue transglutaminase is an inducible enzyme with a variety of physiological functions. It is suggested that tTG plays an important role in the nervous system development, because its activity and expression level change significantly during development. A study from Bailey and Johnson indicated tTG activity increased at the time of brain growth spurt, suggesting that tTG was involved in maturation of the brain [17]. Also, it was demonstrated that tTG was necessary for neurite outgrowth, although its specific role in the formation of neurites in the primary neurons remains to be elucidated [18–20]. Another function of tTG is protein cross-linking. Tissue transglutaminase is a calcium-dependent enzyme that catalyzes an acyl transfer reaction between the γ-carboxamide group of a polypeptide-bound glutamine and the ε-amino group of a polypeptide-bound lysine residue to form a γ-glutamyl-ε-lysine covalent isopeptide bond [21, 22]. The catalyzed isopeptide cross-links can be both intramolecular and intermolecular. Intramolecular cross-linking changes protein

conformation, while intermolecular cross-linking leads to rigid, stable, and highly insoluble protein complexes [23, 24].

Given that tTG cross-linking can cause protein aggregation, it is possible that protein aggregates in AD—extracellular aggregates of Aβ [25, 26] and intracellular aggregates of hyperphosphorylated tau protein [27]—have isopeptide bonds. This suggests that tTG-catalyzed cross-linking of Aβ and tau may contribute to toxic aggregates that contribute to pathogenesis of AD.

Only a few studies have investigated the role of tTG in AD, where evidence suggests that expression and activity are increased in AD comparted to controls [15]. Detailed descriptions of tTG and isopeptide distribution as well as changes in function and regulation are limited. In this study, we report on tTG expression and enzyme activity, as well as neurodegenerative-related proteins in individuals with a range of cognitive impairment and in a transgenic mouse model of AD.

Materials and Methods

Antibodies

Anti-tTG (transglutaminase-2), anti-isopeptide (153-81D4), and anti-paired helical filament type 1 (PHF1) (EPR14222) antibodies were purchased from Abcam (Cambridge, MA). Anti-Aβ (D12B2) antibody was purchased from Cell Signaling Technologies (Danvers, MA). Anti-neurofilament light chain (NF-L), anti-neurofilament medium chain (NF-M), and anti-α-synuclein antibodies were purchased from Covalab (Cambridge, UK). Anti-β-actin, horseradish peroxidase (HRP)- or biotin-conjugated secondary antibodies, and HRP-streptavidin were purchased from ProteinTech (Chicago, IL).

Case and Clinical Feature Data

Brain tissue from frontal cortex was obtained from participants in the Religious Orders Study of the Rush Alzheimer Disease Center (NIH grants P30 AG10161 and R01 AG16819), including ten each of no cognitive impairment (NCI), mild cognitive impairment (MCI), and AD. All individuals had undergone a uniform structured clinical evaluation that included a medical history, neurologic examination, and neuropsychological performance testing. The evaluation included the Mini-Mental State Examination (MMSE) as an overall test of cognition and 20 other cognitive performance tests. Diagnostic classification was performed each year by a team of clinicians. A summary diagnosis was made after death based on review of all clinical data by a neurologist blinded to the neuropathologic assessment. Details of the evaluation have been previously reported [28].

Animals

APPswe/PS1dE9 double transgenic mice (APP/PS1), which express chimeric human/mouse amyloid precursor protein (HuAPP695swe/Mo) and human mutant presenilin 1 (PS1-dE9), as well as wild-type C57 mice (WT) were purchased from Jackson Laboratory. All animal with free access to food and water were raised at room temperature of 23–25 °C, relative humidity of about 50–60 %, and a 12-h:12-h reverse light–dark cycle environment. All

experimental procedures conformed to the guidelines of Care and Use of Laboratory Animals of China for animal experimentation.

Paraffin Section Immunohistochemistry and Quantitative Image Analysis

Paraffin-embedded, glass-mounted sections from persons frontal cortex with NCI, MCI, and AD were processed for immunohistochemistry after deparaffinization in xylenes and rehydration in a series of alcohol washes (100, 100, 95, 75, 50 %). Antigen retrieval was performed with microwave heat-mediated citrate buffer (pH 6.0) for 20 min and return to room temperature (RT). Slices were blocked with endogenous peroxidase blocking buffer (Peroxidazed; Biocare Medical, Concord, CA) and protein block buffer (10 % goat serum in phosphate-buffered saline (PBS)-Triton). Primary antibody was applied (anti-tTG 1:200; anti-isopeptide 1:100) in antibody diluent (Renoir Red; Biocare Medical, Concord, CA) overnight at 4 °C. After rinsing with PBS, biotin-conjugated secondary antibodies were applied for 2 h and HRP-streptavidin for 30 min at RT. tTG or isopeptide was visualized with brown chromogen (Betazoid 3,3'-diaminobenzidine (DAB) Chromogen Kit; Biocare Medical, Concord, CA). Slices were counterstained with hematoxylin, rinsed with distilled water, dehydrated through graded alcohols, and cleared in xylene and permanently coverslipped. Negative controls were performed by replacing the primary antibody with PBS.

Images of sections stained for tTG were captured in the bright-field mode on CRi Nuance imaging system mounted on a microscope, and the average signal intensity was calculated using Nuance version 3.0 software. Images of sections stained for isopeptide were analyzed using Art Spectra Imaging Systems Vectra™ (Caliper Life Sciences, Inc, Hopkinton, MA). Four sections from cortex in each region, with five patients in each group, were analyzed.

Frozen Section Immunohistochemistry of Mice

Frozen sections of mouse brain mounted on glass slices from APP/PS1 transgenic mice (3M (3 months of age), 6M (6 months of age), 9M (9 months of age), 12M (12 months of age)) and WT C57 mice (6 M, 12M) were rehydrated in PBS at RT. All slices were treated for antigen retrieval, and endogenous peroxidase activity was inactivated with 3 % H_2O_2 (methanol/H_2O/30 % H_2O_2=7:2:1) for 15 min. After 1 h of pretreatment, nonspecific antibody binding was blocked with 10 % normal goat serum (diluting in 0.3 % PBS-Triton). Primary antibodies (tTG and isopeptide) in antibody diluent (Renoir Red, Biocare Medical, Concord, CA) were incubated at 4 °C overnight. The slices were exposed to biotin-conjugated secondary antibody for 2 h and HRP-streptavidin for 30 min at RT. tTG and isopeptide were visualized with DAB peroxidase substrate, and sections were counterstained with hematoxylin. Negative controls were performed by replacing the primary antibody with PBS.

Images were taken in bright-field mode on a Nikon microscope and analyzed with Image-Pro Plus 6.0 to calculate integrated optical density (IOD) and area of interest (AOI). The data are expressed as average optical density (IOD/AOI). Regions of interest as defined by a standard mouse atlas [29] are illustrated in Fig. 1. Six sections of cortex and seven sections of hippocampal subregions were captured in each group (three mice in each group).

Western Blot Analysis

Frozen frontal cortex samples from patients (NCI, MCI, AD) and mice (APP/PS1 3M, 6M, 9M, 12M; WT 3M, 6M, 9M, 12M) were homogenized in RIPA buffer (Sigma, St. Louis, M O) with protease inhibitor cocktail and phenylmethanesulfonylfluoride (PMSF) protease inhibitor. Supernatants were collected by centrifuging at 10,000×*g* for 10 min at 4 °C. Protein concentration in the supernatant was determined by BCA kits with bovine serum albumin (BSA) as standard. Samples containing equal amounts of protein were denatured in sample buffer (100 mM Tris–HCl, pH 6.8, 4 % sodium dodecyl sulfate, 0.2 % bromophenol blue, 20 % glycerol, 20 % H_2O, and 200 mM dithiothreitol) at 100 °C for 5 min. Equal amounts of protein were loaded on 10 % SDS-PAGE gel and then transferred to polyvinylidene fluoride (PVDF) membranes (Millipore, Billerica, MA). The membranes were blocked in Tris-buffered saline with 0.05 % Tween (TBST) containing 5 % non-fat milk for 1 h at RT before incubation with primary antibodies (tTG, 1:2,000; isopeptide, 1:500; β-actin, 1:10,000) overnight at 4 °C followed by 3×10 min washes in TBST. Immunodetection was performed using HRP-conjugated secondary antibodies. The antibody binding was visualized with electrochemiluminescence (ECL) and detected on BioImaging System (DNR Lumi BIS, Jerusalem, Israel). The densities of target bands were determined by Image-Pro Plus 6.0 and expressed as relative level with respect to the loading control β-actin.

Co-localization of Isopeptide and Potential Neurodegenerative-Related Proteins

Frozen tissue samples from cerebral cortex of humans and mice were homogenized and centrifuged. Samples were loaded and separated with 12 % Tris-glycine polyacrylamide gels and transferred to PVDF membranes. After blocking with TBST containing 5 % non-fat milk, the membranes were kept at 4 °C overnight with primary antibody, followed by HRP-conjugated second antibodies at RT for 2 h. The target protein bands were detected using the ECL Western blotting detection system (DNR Lumi BIS). After first blotting with anti-isopeptide antibody (1:500), the membranes were stripped in stripping buffer three times (10 min each) at 50 °C, then membranes were washed with TBST three times (10 min each) at RT. After blocking with TBST containing 5 % non-fat milk, the membranes were re-blotted with second primary antibodies (Aβ, α-synuclein, PHF1, NF-L, NF-M; all at 1:1,000) at 4 °C overnight. The following steps were similar to isopeptide detection. Using pseudo-color technology, we merged the whole panels of isopeptide and cross-linked substrate proteins, in order to show overlap of isopeptide and potential substrate proteins.

Statistical Analyses

All data were expressed as mean±standard error of the mean (SEM) or median. Statistical analyses were performed with one-way ANOVA followed by least significant difference post hoc analysis (multiple comparisons) and linear regression analysis with threshold of $P<0.05$ on SPSS Statistics 17.0 software. The results from individual experiments were averaged within each experimental group.

Results

tTG Levels Are Higher in AD

To confirm tTG protein level differences in NCI, MCI, and AD brains, we first performed immunohistochemistry for tTG antibody with CRi Nuance imaging system with wavelength-resolved imaging (Fig. 2A, a–c) and data acquisition (Fig. 2A, d). The results showed that tTG protein level was significantly increased in AD and that tTG was mainly located in the cytoplasm of cells. Extracellular levels also appeared to be increased in AD. We also detected tTG biochemically with Western blot analysis (Fig. 2B). Specific bands at ~77–85 kDa reacted with anti-tTG. Densitometric analysis of these bands showed a significant increase in AD.

tTG Protein Expression Increases with Age in a Transgenic Model of AD

In order to observe changes in tTG with age, we studied brains of APP/PS1 transgenic mice with immunohistochemistry and Western blotting at 3, 6, 9, and 12 months of age. The density of tTG immunoreactivity was visualized by image analysis of cerebral cortex (Fig. 3A, a, b, d, e) and hippocampus (Fig. 3B, a, b, d, e). Immunoreactivity was present in both regions and decreased slightly in 12M APP/PS1 transgenic mice. An uneven distribution was observed in hippocampus. Some plaque-like staining appeared in APP/PS1 mice at 9M and then increased at 12M. Immunoreactivity in nuclei, counterstained with hematoxylin, decreased at 12M compared with 9M. Nuclear immunoreactivity detected in CA1 and CA3 was less than in the DG. Cytoplasmic staining of tTG was uniform at 3M and 6M but tended to be concentrated around plaques at 9M, especially in hippocampal subregions.

Image analysis quantification (Fig. 3C, a) showed similar trends to subjective assessment in cortex and hippocampus. In cortex, the most significant increase in tTG immunoreactivity was observed at 9M compared to 3M ($P<0.001$), 6M, and 12M ($P<0.01$). In hippocampus, tTG increased significantly at 9M ($P<0.001$) and 12M ($P<0.01$). The tTG immunoreactivity in hippocampus was lower than in cortex at each time point, reaching statistical significance at 6M ($P<0.05$). Because of uneven distribution in hippocampus, we also evaluated tTG immunoreactivity in CA1, CA3, and DG subregions, separately. Interestingly, tTG showed higher expression in CA3 and DG than in CA1 (Fig. 3C, b).

To study the effects of age, we measured immunoreactivity of tTG in mature adult (6M) and aged mice (12M). Analysis of cortex (Fig. 3A, b, c, e, f), hippocampus (Fig. 3B, b, c, e, f), and total immunoreactivity (Fig. 3C, c) showed few differences between WT and APP/PS1 mice at 6M but significant increases in APP/PS1 in cortex ($P<0.001$) and hippocampus ($P<0.01$) at 12M. Hippocampal subregions (CA1, CA3, and DG) showed different densities of tTG immunoreactivity (Fig. 3C, d), so they were analyzed separately. At 6M of age, APP/PS1 showed slight decreases compared to WT mice but significant increases at 12M. At 6M of age, there were no differences in tTG immunoreactivity in CA3 and DG, but APP/PS1 had significant increases in both areas ($P<0.05$, $P<0.01$) at 12M.

To confirm immunohistochemistry results, tTG levels were assessed with Western blotting at 3M, 6M, 9M, and 12M of APP/PS1 and WT mice. Similar to immunohistochemistry, tTG protein increased with age in APP/PS1 mice, and it was lower in 6M WT mice. When

compared to WT mice, APP/PS1 had significance increases at 9M (P<0.05) and greater at 12M (P<0.001) (Fig. 3D).

Isopeptide Levels Are Higher in MCI and AD

To assess if there are progressive changes in isopeptides in cerebral cortex of NCI, MCI, and AD, we performed immunohistochemistry using an anti-isopeptide antibody and quantification with art spectra imaging systems (Vectra™). Isopeptide immunoreactivity was detected in both the nuclei and cytoplasm/plasma membrane of cells in the neocortex (primary images were not shown) (Fig. 4a). There was no difference in levels of nuclear isopeptide immunoreactivity between NCI, MCI, and AD. On the other hand, increases in cytoplasm/plasma membrane immunoreactivity were detected in AD and MCI compared to NCI. Interestingly, isopeptide immunoreactivity was increased in MCI relative to both NCI and AD for cytoplasm/plasma membrane (P<0.01) and for total immunoreactivity (nucleus and cytoplasm/plasma membrane (P<0.001)).

We also measured total isopeptide protein level in cortex by Western blotting with anti-isopeptide antibody. Using ECL imaging, isopeptide relative levels were quantified by Image-Pro Plus 6.0. Analyses showed (Fig. 4b) that isopeptide levels were increased in MCI and AD compared to NCI, and the differences were statistically significant in AD (P<0.05).

Protein Cross-Linking Level Increased with Age in Transgenic Model Mice of AD

Isopeptide immunohistochemistry was measured in APP/PS1 mice in neocortex (Fig. 5A, a, b, d, e) and hippocampus (Fig. 5B, a, b, d, e). Increased immunoreactivity with age was obvious in both regions, but it decreased slightly at 12M. The hippocampal immunoreactivity was uneven, isopeptide immunoreactivity mainly in cytoplasm/plasma membrane at 6M, while plaque-like staining appeared at 9M and increased in 12M mice. Nuclear isopeptide immunoreactivity, as detected with hematoxylin counterstains, decreased at 12M, especially in the hippocampus. In addition, CA3 and DG hippocampal subregions showed more immunoreactivity than the CA1 in 9M mice.

Isopeptide immunoreactivity was quantified with image analysis, which showed increased isopeptide in APP/PS1 mice from 6M to 9M (Fig. 5C, a), decreasing slightly at 12M. In cortex, isopeptide levels were increased at 9M (P<0.001) and 12M (P<0.05) compared with 3M mice. Only 9M had significant increase in the hippocampus (P<0.05). Interestingly, immunoreactivity in cortex was greater than hippocampus at each age, most marked at 9M (P<0.05). Isopeptide immunoreactivity was uneven in the hippocampus, so we analyzed isopeptide immunoreactivity in CA1, CA3, and DG separately. Isopeptide levels were high DG and CA3 but lower in CA1 (Fig. 5C, b).

To exclude influence of aging, we measured isopeptide immunoreactivity in mature (6M) and aged (12M) WT and APP/PS1 mice. The isopeptide levels did not differ between WT and APP/PS1 mice in cortex (Fig. 5A, b, c, e, f) and hippocampus (Fig. 5B, b, c, e, f) or combined (Fig. 5C, c) at 6M, but there was a significant increase in isopeptide in cortex (P<0.001) and hippocampus (P<0.001) in APP/PS1 mice compared to WT at 12M. Differences were detected in hippocampal subregions (Fig. 5C, d). In CA1, APP/PS1 was

not different from WT at 6M, but it was greater at 12M ($P<0.001$). In CA3 and DG, APP/PS1 showed a mild increase at 6M ($P<0.05$) but greater increases at 12M ($P<0.001$).

To further confirm immunohistochemistry results, Western blotting was used to measured isopeptide levels at 3M, 6M, 9M, and 12M of both APP/PS1 and WT mice. Consistent with immunohistochemistry, isopeptide protein increased with age in APP/PS1 mice, with significant differences at 12M ($P<0.01$). Compared to WT, APP/PS1 had increases at 9M ($P<0.05$) and 12M ($P<0.001$) (Fig. 5D).

Neurodegeneration-Related Proteins in AD

To analyze differences in isopeptide levels with respect to changes in proteins implicated in neurodegeneration, we performed Western blots of isopeptide as well as Aβ (Fig. 6a–c), α-synuclein (Fig. 6d–f), phosphorylated tau protein (PHF1 (Fig. 6g–i)), intermediate filament proteins (NF-L (Fig. 6j–l), and NF-M (Fig. 6m–o)) in NCI, MCI, and AD brains using the same PVDF membrane. To observe the relationship between isopeptide and potential cross-linking substrates, we used pseudo-color technology on immunoblotting images. Isopeptide (red) and potential substrate proteins (green) were merged (yellow) to show the overlap.

Compared to NCI, both MCI and AD brains had higher levels of Aβ levels (Fig. 6a). Moreover, there were three prominent bands in MCI and AD brains, with one of the bands at ~50 kDa, and the others between 35 and 50 kDa (Fig. 6c).

Monomer α-synuclein (15 kDa) was apparent in NCI and some MCI brains, but it was lower in AD in this small sample. Oligomers were the major immunoreactive species of α-synuclein in AD (Fig. 6d). There was little evidence of overlap between isopeptide and α-synuclein immunoreactivities (Fig. 6f).

Although phosphorylated tau (PHF1) bands (located at ~43, ~55, ~65, ~90 kDa) were only detected in one AD and two MCI samples (Fig. 6g), there was overlap of signals for isopeptide and PHF1 in these three samples (Fig. 6i). The isopeptide signal was stronger than the PHF1 signal in the negative samples.

NF-L bands (located at ~65, ~70, ~90, ~180, ~200 kDa) were increased in AD compared to NCI and MCI (Fig. 6j). Isopeptide immunoreactivity overlapped at ~65, ~70, and ~90 kDa in AD but only at ~90 kDa in MCI (Fig. 6l).

NF-M bands (located at ~30, ~40, ~105, ~170 kDa) were increased in AD compared to NCI and MCI (Fig. 6m). Isopeptide immunoreactivity overlapped at ~30, ~40, and ~105 kDa in AD brains (Fig. 6o).

In summary, isopeptide immunoreactivity overlapped with protein bands on immunoblots of Aβ, phospho-tau (PHF-1), and neurofilament (NF-L, NF-M) in both MCI and AD brains. By contrast, immunoreactive bands for α-synuclein did not seem overlap with isopeptide immunoreactive bands.

Neurodegenerative-Related Proteins in AD Model Mice Brains

We used a similar analysis to determine how isopeptide immunoreactive bands overlap with neurodegenerative proteins in APP/PS1 and WT mice at various ages. Specifically, we looked for overlap of isopeptide immunoreactivity with Aβ (Fig. 7a–c), α-synuclein (Fig. 7d–f), PHF-1 (Fig. 7g–i), NF-L (Fig. 7j–l), and NF-M (Fig. 7m–o). As in human samples, immunoreactivities for isopeptide (red) and neurodegeneration-associated proteins (green) were merged (yellow) to show overlap.

There were significant increases of Aβ in APP/PS1 mice at 9M and 12M (Fig. 7a). The signals of tetramer at ~16 kDa and oligomers above ~200 kDa were much stronger than bands between 25 and 170 kDa. Compared to WT mice, total Aβ was much higher in APP/PS1 mice, increasing gradually with age. Isopeptide immunoreactivity was detectable in all samples, with higher levels in aged APP/PS1 mice. The most overlap with isopeptide was at ~35, ~40, ~45, ~55, ~100, and ~130 kDa (Fig. 7c).

Immunoreactive α-synuclein was observed at ~15 kDa (monomer) and ~45 kDa (trimer) with no obvious difference between WT and APP/PS1 or with age (Fig. 7d). There was also no overlap with isopeptide immunoreactivity (Fig. 7f).

Similar to AD, phosphorylated tau PHF1 was higher in APP/PS1 mice, and overlap was detected with isopeptide immunoreactivity (Fig. 7g–i). NF-L and NF-M were both higher in APP/PS1 compared to WT mice. There was greater overlap with isopeptide immunoreactivity in aged APP/PS1 compared to WT mice (Fig. 7j–o).

The results suggest that isopeptide cross-linking might be occurring in Aβ, Tau, and neurofilament proteins in APP/PS1 mice, similar to that observed in human brains.

Discussion

It has been ever hypothesized that multi-factors such as trauma [30, 31], inflammation [32, 33], or ischemic damage [34, 35] in sporadic AD or overproduction of Aβ in familial AD might lead to cross-linking of AD-related proteins. The overproduction of tTG-catalyzed protein cross-linking in turn aggravates the pathogenesis of AD progress [15]. tTG can covalently cross-link AD-related proteins including Aβ and Tau into stable and insoluble polymers by forming γ-glutamyl-ε-lysine isopeptide. Highly resistant to proteolysis, this bond can induce protein aggregation and deposition. Thus, tTG may play an important role in AD.

Previous studies have found higher levels of tTG protein or enzyme activity levels in AD compared to controls [15, 36, 14]. Consistent with others, both immunohistochemical and immunoblot data showed significant increases of tTG in AD. In addition, isopeptide levels were increased in MCI compared to NCI. The greater isopeptide immunoreactivity in MCI suggests that tTG activity is involved in early stages of the pathogenesis of AD. Much of tTG immunoreactivity was located in cytoplasm/plasma membrane in NCI and MCI, but it translocated to extracellular space in AD. A similar phenomenon occurred with isopeptide

immunohistochemistry (not shown). Plaque-like structures were detected in AD with isopeptide immunohistochemistry.

Studies of human tissue are by nature cross-sectional, and one can only infer longitudinal processes. To overcome this limitation, we also performed the same experiments in a transgenic mouse model of AD to detect dynamic changes in tTG, isopeptide, and potential substrate proteins. We found that tTG expression and isopeptide levels increase with age in a transgenic model of AD, with the most robust changes occurring in the hippocampus, a region of the brain vulnerable to Alzheimer type pathologic changes [37, 38].

Interestingly, obvious uneven distribution of them was observed in hippocampal subregions in our data. Less tTG and isopeptide in CA1 region were detected intracellularly, but much more tTG and isopeptide were in CA3 and DG regions intra- and extracellularly, and they gradually increased with age. Hippocampus plays important roles in the consolidation of information from short-term memory to long-term memory and spatial navigation [39, 40]. This function is involved in the hippocampal detection of novel events, places, and stimuli [41]. Damage of hippocampus had influence on the forming of new memories, but older memories before the damage can be retained [42, 43]. Pyramidal neurons in the CA1 region of the hippocampus are highly vulnerable to damage from hypoxia-ischemia, whereas neurons in the CA3 region and the dentate gyrus are more resistant [44, 45]. In present study, accumulation of tTG and isopeptide in CA3 and DG regions might imply some connection with the difference in their vulnerable to damage.

Neuronal loss is a typical feature in AD as reported [46, 47]. Our data showed a sharply reduced of cell numbers in aged mice brains, especially in hippocampal CA1 and CA3 subregions. There is evidence suggesting that apoptotic cell death is a feature of AD pathogenesis [48–50]. We hypothesize that neuron death releases proteins into extracellular space, which might trigger removal or clearance mechanisms. Extracellular tTG, like other members of the TG member, such as factor XIII-A [51, 52], may cross-link these extracellular proteins to facilitate clearance, but at the same time lead to progressive accumulation as their formation outstrips clearance mechanisms. Whether tTG might act on intracellular proteins, such as Aβ, and promote their transfer to the extracellular compartment needs to be studied, as well. As explained above, plaque-like positive staining, uneven distribution in partial sections, and death of neurons may be the reasons why tTG and isopeptide levels in AD patients or aged APP/PS1 mice reduce slightly.

The role of tTG in neurofibrillary pathology has been suggested for many years [53]. It has been shown to cross-link tau protein into anti-parallel dimers that may eventually lead to filament formation in NFTs [54]. In addition, tTG immunoreactivity has been observed in NFTs in AD [55–57, 27]. Other insoluble protein aggregates, such as α-synuclein, can also be cross-linked by tTG [58, 59].

In present study, we detected isopeptide immunoreactivity co-localization on immunoblots of AD brain with several neurodegenerative related proteins, namely Aβ, tau (PHF1), and neurofilament (NF-L, NF-M) but not α-synuclein. The degree of co-localization was variable from case-to-case but showed tendency to increase in MCI and AD compared to

NCI. In addition, the molecular weights of the bands that showed co-localization were higher than the weights predicted by the native proteins. Further studies are needed to determine the relationship between neuropathologic and clinical features of cases with isopeptide co-location compared to cases where there was minimal isopeptide immunoreactivity. For extracellular deposits, such as Aβ, it will be of interest to learn if the cross-linking occurs in the intracellular or extracellular compartment or both.

Conclusion

Increasing evidence suggests that tTG plays an important role in the pathogenesis of AD. Its main enzyme activity is to catalyze γ-glutamyl-ε-lysine cross-links within or between proteins. Previous studies explored tTG expression and enzyme activity in AD compared to NCI, but the timing of this process was not known. In the present study, we included subjects with MCI as a transition state between NCI and AD [12] and find that some MCI patients have increased tTG and isopeptide compared to NCI. We also studied the timing issue in a mouse model of AD and find age-related increases in tTG and isopeptide, as well as notable changes in cellular compartments, with formation of extracellular plaque-like lesions in APP/PS1 mice at older ages. In contrast, the levels seem to decrease in WT mice. We also showed uneven distribution in hippocampus which may shed light on selective vulnerability of subregions of the hippocampus to neurodegenerative processes. Finally, we showed that not only Aβ and tau are substrates from increasing cross-linking in AD but also key structural elements of the cytoskeleton, namely neurofilament proteins. The consequences of cross-linking of neurofilament in MCI and AD on axonal integrity require further study. These observations indicated not only that tTG may play a role in pathogenesis of AD by cross-linking proteins that form intracellular and extracellular aggregates but also opens up a new disease target and novel therapies for AD.

Acknowledgments

This work was supported by the grants to Rui Wang from the National Natural Science Foundation of China (81072627); Shanghai Committee of Science and Technology (12431900901); 111 Project of Chinese Ministry of Education (Grant No. B07023); grants AG025722 and AG029972 to Dengshun Wang from the National Institutes of Health (NIH); and an Alzheimer's Association grant IIRG-08-90524. The human samples used in this study are from NIH grants to David Bennett (P30AG10161, R01AG15819).

References

1. Selkoe DJ. The molecular pathology of Alzheimer's disease. Neuron. 1991; 6(4):487–498. [PubMed: 1673054]
2. Dickson D. Neuropathological diagnosis of Alzheimer's disease: a perspective from longitudinal clinicopathological studies. Neurobiol Aging. 1997; 18(4):S21–S26. [PubMed: 9330981]
3. Selkoe DJ. Aging, amyloid, and Alzheimer's disease: a perspective in honor of Carl Cotman. Neurochem Res. 2003; 28(11):1705–1713. [PubMed: 14584824]
4. Greenberg SM, Vonsattel J, Stakes J, Gruber M, Finklestein S. The clinical spectrum of cerebral amyloid angiopathy presentations without lobar hemorrhage. Neurology. 1993; 43(10):2073–2073. [PubMed: 8413970]
5. Tian J, Shi J, Mann D. Cerebral amyloid angiopathy and dementia. Panminerva Med. 2004; 46(4): 253–264. [PubMed: 15876981]

6. Kokubo H, Kayed R, Glabe CG, Yamaguchi H. Soluble Aβ oligomers ultrastructurally localize to cell processes and might be related to synaptic dysfunction in Alzheimer's disease brain. Brain Res. 2005; 1031(2):222–228. [PubMed: 15649447]
7. Wilcock DM, Rojiani A, Rosenthal A, Subbarao S, Freeman MJ, Gordon MN, Morgan D. Passive immunotherapy against Aβ in aged APP-transgenic mice reverses cognitive deficits and depletes parenchymal amyloid deposits in spite of increased vascular amyloid and microhemorrhage. J Neuroinflammation. 2004; 1(1):24. [PubMed: 15588287]
8. Gurol M, Irizarry M, Smith E, Raju S, Diaz-Arrastia R, Bottiglieri T, Rosand J, Growdon J, et al. Plasma β-amyloid and white matter lesions in AD, MCI, and cerebral amyloid angiopathy. Neurology. 2006; 66(1):23–29. [PubMed: 16401840]
9. Herzig MC, Winkler DT, Burgermeister P, Pfeifer M, Kohler E, Schmidt SD, Danner S, Abramowski D, et al. Aβ is targeted to the vasculature in a mouse model of hereditary cerebral hemorrhage with amyloidosis. Nat Neurosci. 2004; 7(9):954–960. [PubMed: 15311281]
10. Lee V, Balin BJ, Otvos L, Trojanowski JQ. A68: a major subunit of paired helical filaments and derivatized forms of normal Tau. Science. 1991; 251(4994):675–678. [PubMed: 1899488]
11. Duyckaerts C. Looking for the link between plaques and tangles. Neurobiol Aging. 2004; 25(6): 735–739. [PubMed: 15165696]
12. Jack CR Jr, Knopman DS, Jagust WJ, Petersen RC, Weiner MW, Aisen PS, Shaw LM, Vemuri P, et al. Tracking pathophysio-logical processes in Alzheimer's disease: an updated hypothetical model of dynamic biomarkers. Lancet Neurol. 2013; 12(2):207–216. doi: 10.1016/S1474-4422(12)70291-0. [PubMed: 23332364]
13. Wilhelmus MM, van Dam A-M, Drukarch B. Tissue transglutaminase: a novel pharmacological target in preventing toxic protein aggregation in neurodegenerative diseases. Eur J Pharmacol. 2008; 585(2):464–472. [PubMed: 18417122]
14. Kim S-Y, Grant P, Lee J-H, Pant HC, Steinert PM. Differential expression of multiple transglutaminases in human brain Increased expression and cross-linking by transglutaminases 1 and 2 in Alzheimer's disease. J Biol Chem. 1999; 274(43):30715–30721. [PubMed: 10521460]
15. Wang D-S, Uchikado H, Bennett DA, Schneider JA, Mufson EJ, Wu J, Dickson DW. Cognitive performance correlates with cortical isopeptide immunoreactivity as well as Alzheimer type pathology. J Alzheimers Dis. 2008; 13(1):53–66. [PubMed: 18334757]
16. Lesort M, Attanavanich K, Zhang J, Johnson GV. Distinct nuclear localization and activity of tissue transglutaminase. J Biol Chem. 1998; 273(20):11991–11994. [PubMed: 9575137]
17. Bailey CD, Johnson GV. Developmental regulation of tissue transglutaminase in the mouse forebrain. J Neurochem. 2004; 91(6):1369–1379. [PubMed: 15584913]
18. Mahoney S-A, Wilkinson M, Smith S, Haynes L. Stabilization of neurites in cerebellar granule cells by transglutaminase activity: identification of midkine and galectin-3 as substrates. Neuroscience. 2000; 101(1):141–155. [PubMed: 11068143]
19. Tucholski J, Lesort M, Johnson G. Tissue transglutaminase is essential for neurite outgrowth in human neuroblastoma SH-SY5Y cells. Neuroscience. 2001; 102(2):481–491. [PubMed: 11166134]
20. Singh US, Pan J, Kao Y-L, Joshi S, Young KL, Baker KM. Tissue transglutaminase mediates activation of RhoA and MAP kinase pathways during retinoic acid-induced neuronal differentiation of SH-SY5Y cells. J Biol Chem. 2003; 278(1):391–399. [PubMed: 12401808]
21. Greenberg CS, Birckbichler PJ, Rice RH. Transglutaminases: multifunctional cross-linking enzymes that stabilize tissues. FASEB J. 1991; 5(15):3071–3077. [PubMed: 1683845]
22. Aeschlimann, D.; Mosher, D.; Paulsson, M. Seminars in thrombosis and hemostasis. Vol. 05. Copyright© 1996 by Thieme Medical Publishers, Inc.; 1996. Tissue transglutaminase and factor XIII in cartilage and bone remodeling.; p. 437-443.
23. Lorand, L.; Conrad, SM. Transglutaminase. Springer; 1984. Transglutaminases.; p. 9-35.
24. Folk J. The trimethylacetyl-transglutaminase complex. Methods Enzymol. 1981; 87:36–42. [PubMed: 6129561]
25. Zhang J, Lesort M, Guttmann RP, Johnson GV. Modulation of the in situ activity of tissue transglutaminase by calcium and GTP. J Biol Chem. 1998; 273(4):2288–2295. [PubMed: 9442073]

26. Zhang W, Johnson BR, Suri DE, Martinez J, Bjornsson TD. Immunohistochemical demonstration of tissue transglutaminase in amyloid plaques. Acta Neuropathol. 1998; 96(4):395–400. [PubMed: 9797004]
27. Singer SM, Zainelli GM, Norlund MA, Lee JM, Muma NA. Transglutaminase bonds in neurofibrillary tangles and paired helical filament tau early in Alzheimer's disease. Neurochem Int. 2002; 40(1):17–30. [PubMed: 11738469]
28. Bennett DA. Overview and findings from the religious orders study. Current Alzheimer Research. 2012; 9
29. Paxinos, G.; Franklin, KB. The mouse brain in stereotaxic coordinates. Gulf Professional Publishing; 2004.
30. Fleminger S, Oliver D, Lovestone S, Rabe-Hesketh S, Giora A. Head injury as a risk factor for Alzheimer's disease: the evidence 10 years on; a partial replication. J Neurol Neurosurg Psychiatry. 2003; 74(7):857–862. [PubMed: 12810767]
31. Szczygielski J, Mautes A, Steudel W, Falkai P, Bayer T, Wirths O. Traumatic brain injury: cause or risk of Alzheimer's disease? A review of experimental studies. J Neural Transm. 2005; 112(11): 1547–1564. [PubMed: 15959838]
32. Sastre M, Klockgether T, Heneka MT. Contribution of inflammatory processes to Alzheimer's disease: molecular mechanisms. Int J Dev Neurosci. 2006; 24(2):167–176. [PubMed: 16472958]
33. Rogers JT, Lahiri DK. Metal and inflammatory targets for Alzheimer's disease. Curr Drug Targets. 2004; 5(6):535–551. [PubMed: 15270200]
34. Rosano C, Newman AB. Cardiovascular disease and risk of Alzheimer's disease. Neurol Res. 2006; 28(6):612–620. [PubMed: 16945212]
35. Koistinaho M, Koistinaho J. Interactions between Alzheimer's disease and cerebral ischemia—focus on inflammation. Brain Res Rev. 2005; 48(2):240–250. [PubMed: 15850663]
36. Johnson GV, Cox TM, Lockhart JP, Zinnerman MD, Miller ML, Powers RE. Transglutaminase activity is increased in Alzheimer's disease brain. Brain Res. 1997; 751(2):323–329. [PubMed: 9099822]
37. Braak H, Braak E. Neuropathological stageing of Alzheimer-related changes. Acta Neuropathol. 1991; 82(4):239–259. [PubMed: 1759558]
38. Thal DR, Rub U, Orantes M, Braak H. Phases of A beta-deposition in the human brain and its relevance for the development of AD. Neurology. 2002; 58(12):1791–1800. [PubMed: 12084879]
39. Moser M-B, Moser EI. Functional differentiation in the hippocampus. Hippocampus. 1998; 8:608–619. [PubMed: 9882018]
40. Tulving E, Markowitsch HJ. Episodic and declarative memory: role of the hippocampus. Hippocampus. 1998; 8(3)
41. VanElzakker M, Fevurly RD, Breindel T, Spencer RL. Environmental novelty is associated with a selective increase in Fos expression in the output elements of the hippocampal formation and the perirhinal cortex. Learn Mem. 2008; 15(12):899–908. [PubMed: 19050162]
42. Moscovitch M, Winocur G. The neuropsychology of memory and aging. 1992
43. Eichenbaum, H. Memory, amnesia, and the hippocampal system. MIT Press; Cambridge: 1993.
44. Watanabe Y, Gould E, McEwen BS. Stress induces atrophy of apical dendrites of hippocampal CA3 pyramidal neurons. Brain Res. 1992; 588(2):341–345. [PubMed: 1393587]
45. Becker AJ, Gillardon F, Blümcke I, Langendörfer D, Beck H, Wiestler OD. Differential regulation of apoptosis-related genes in resistant and vulnerable subfields of the rat epileptic hippocampus. Mol Brain Res. 1999; 67(1):172–176. [PubMed: 10101244]
46. Luo L, O'Leary DD. Axon retraction and degeneration in development and disease. Annu Rev Neurosci. 2005; 28:127–156. [PubMed: 16022592]
47. Heggland I, Storkaas IS, Soligard HT, Kobro-Flatmoen A, Witter MP. Stereological estimation of neuron number and plaque load in the hippocampal region of a transgenic rat model of Alzheimer's disease. Eur J Neurosci. 2015
48. Bayer AU, Keller ON, Ferrari F, Maag K-P. Association of glaucoma with neurodegenerative diseases with apoptotic cell death: Alzheimer's disease and Parkinson's disease. Am J Ophthalmol. 2002; 133(1):135–137. [PubMed: 11755850]

49. Yang Y, Mufson EJ, Herrup K. Neuronal cell death is preceded by cell cycle events at all stages of Alzheimer's disease. J Neurosci. 2003; 23(7):2557–2563. [PubMed: 12684440]
50. Yang Y, Geldmacher DS, Herrup K. DNA replication precedes neuronal cell death in Alzheimer's disease. J Neurosci. 2001; 21(8):2661–2668. [PubMed: 11306619]
51. Keski-Oja J, Mosher DF, Vaheri A. Cross-linking of a major fibroblast surface-associated glycoprotein (fibronectin) catalyzed by blood coagulation factor XIII. Cell. 1976; 9(1):29–35. [PubMed: 975239]
52. Schwartz ML, Pizzo SV, Hill RL, McKee PA. Human factor XIII from plasma and platelets molecular weights, subunit structures, proteolytic activation, and cross-linking of fibrinogen and fibrin. J Biol Chem. 1973; 248(4):1395–1407. [PubMed: 4405643]
53. Selkoe DJ, Abraham C, Ihara Y. Brain transglutaminase: in vitro crosslinking of human neurofilament proteins into insoluble polymers. Proc Natl Acad Sci U S A. 1982; 79(19):6070–6074. [PubMed: 6136967]
54. Prasanna Murthy S, Wilson JH, Lukas TJ, Kuret J, Lorand L. Cross-linking sites of the human Tau protein, probed by reactions with human transglutaminase. J Neurochem. 1998; 71(6):2607–2614. [PubMed: 9832162]
55. Wilhelmus MM, Grunberg S, Bol JG, Van Dam AM, Hoozemans JJ, Rozemuller AJ, Drukarch B. Transglutaminases and transglutaminase-catalyzed cross-links colocalize with the pathological lesions in Alzheimer's disease brain. Brain Pathol. 2009; 19(4):612–622. [PubMed: 18673368]
56. Citron BA, Suo Z, SantaCruz K, Davies PJ, Qin F, Festoff BW. Protein crosslinking, tissue transglutaminase, alternative splicing and neurodegeneration. Neurochem Int. 2002; 40(1):69–78. [PubMed: 11738473]
57. Wilhelmus MM, de Jager M, Rozemuller AJ, Brevé J, Bol JG, Eckert RL, Drukarch B. Transglutaminase 1 and its regulator tazarotene-induced gene 3 localize to neuronal tau inclusions in tauopathies. J Pathol. 2012; 226(1):132–142. [PubMed: 22009441]
58. Andringa G, Lam K, Chegary M, Wang X, Chase T, Bennett M. Tissue transglutaminase catalyzes the formation of alpha-synuclein crosslinks in Parkinson's disease. FASEB J. 2004; 18(7):932–934. [PubMed: 15001552]
59. Verhaar R, Jongenelen CA, Gerard M, Baekelandt V, Van Dam AM, Wilhelmus MM, Drukarch B. Blockade of enzyme activity inhibits tissue transglutaminase-mediated transamidation of alpha-synuclein in a cellular model of Parkinson's disease. Neurochem Int. 2011; 58(7):785–793. doi: 10.1016/j.neuint.2011.03.004. [PubMed: 21440023]

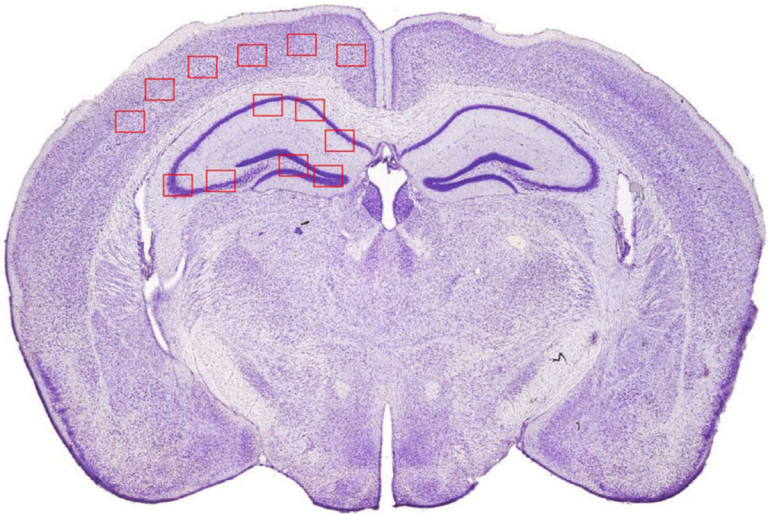

Fig. 1.

Mouse brain diagram. Diagram of cortex and hippocampus sections of mouse brain (interaural 1.86 mm, bregma −1.94 mm) showing the locations of sampling in different brain regions for immunohistochemistry quantitative analysis. Cortical sections were from parietal lobe along the contour extension. Three from CA1 region, two from CA3 region, and two from DG region of hippocampal sections were captured for the analysis

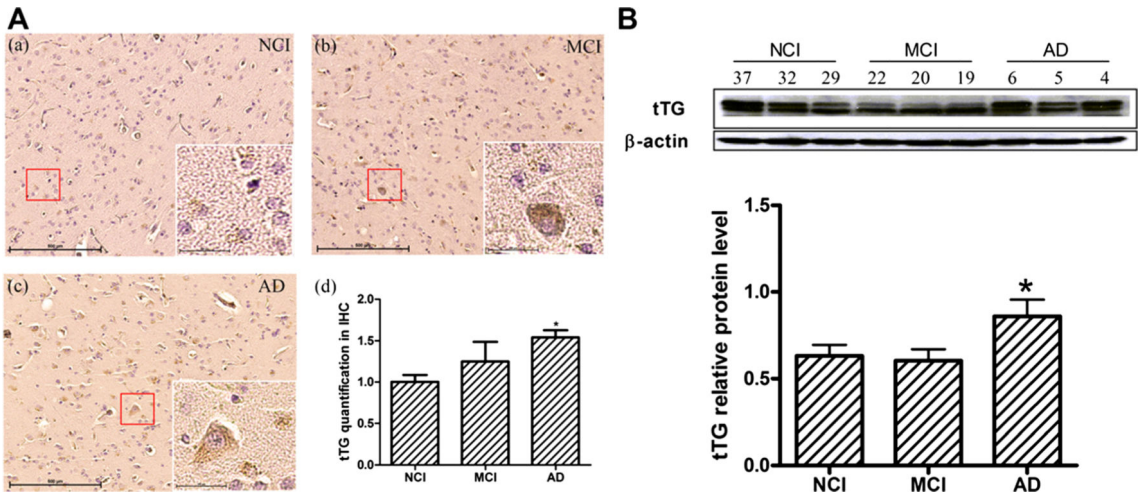

Fig. 2.

Alterations of tTG in NCI, MCI, and AD brains. **A** Immunohistochemistry of tTG quantification level by SP-DAB method in NCI (*a*), MCI (*b*), and AD (*c*). Four sections from cortex in each region with five patients in each group were analyzed. CRi Nuance imaging system was mounted on a microscope for wavelength-resolved imaging and data acquisition from tTG slices. Imaging was done in the bright-field mode via CRi Nuance imaging system, and the average signal intensity of tTG in the cortex was calculated by using Nuance version 3.0 software.

Figure is the representative photos of tTG with ×100 and ×400 magnification. **B** Western blotting of tTG relative level with β-actin in NCI, MCI, and AD (n=10 for each group). Images were detected on Bio Imaging System (DNR) via ECL system and analyzed by Image-Pro Plus 6.0 software. Figure is the representative bands of tTG and β-actin Western blotting. Statistical data expressed as mean±SEM from three independent experiments group.* P<0.05 vs. NCI group

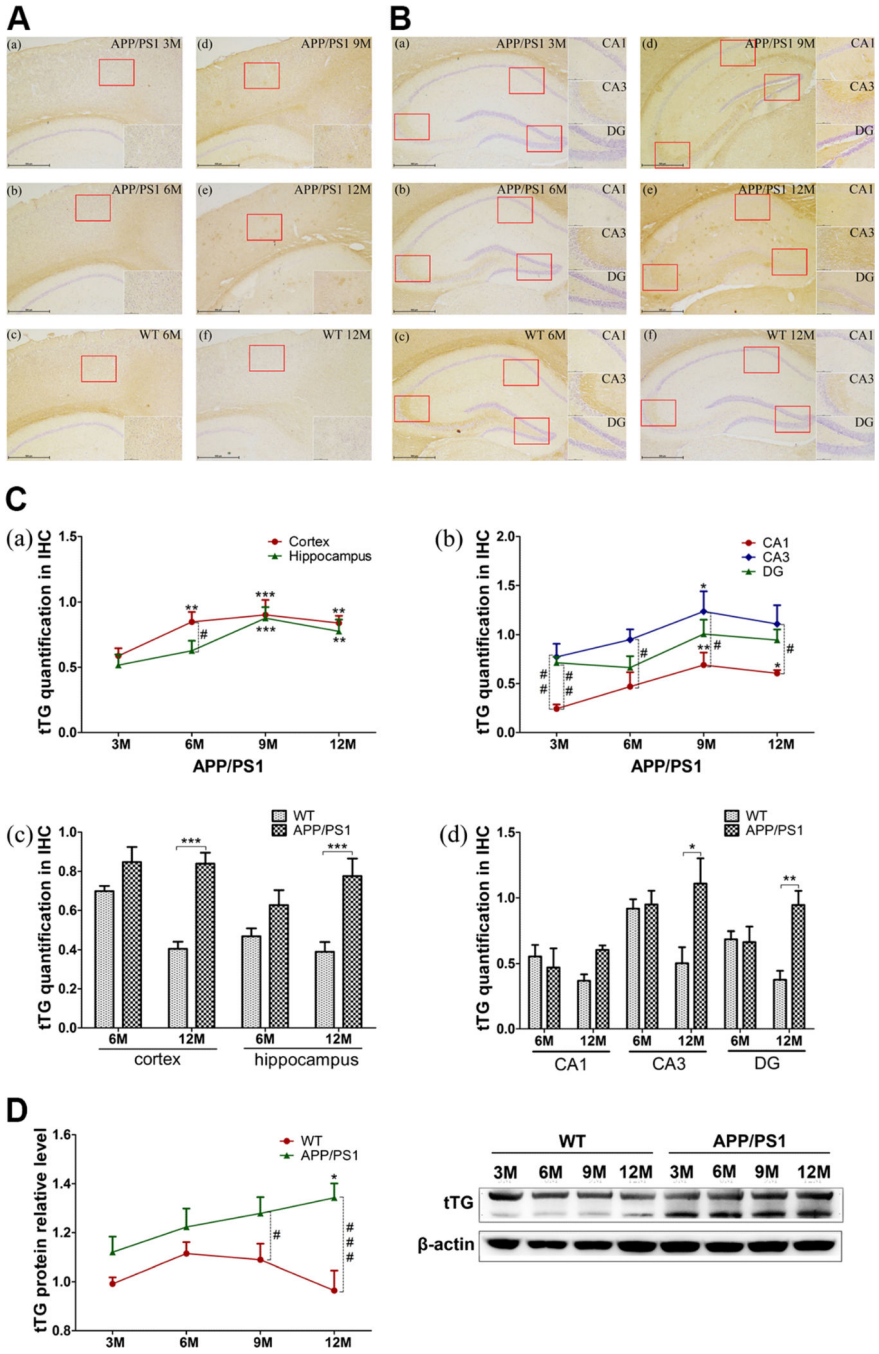

Fig. 3.

Alterations of tTG in APP/PS1 and WT mice. **A, B** Immunohistochemistry of tTG quantification level by SP-DAB method in 3M (*a*), 6M (*b*), 9M (*d*), and 12M (*e*) APP/PS1 transgenic mice or 6M (*c*), 12M (*f*) WT mice cortex (**A**), and hippocampus (**B**). The repres entative photos of tTG with ×40 and ×200 magnification are shown. **C** Data acquisition from tTG slices. The average signal intensity (IOD/AOI) of tTG in the cortex and hippocampus was calculated by using Image-Pro Plus 6.0 software. Six sections from cortex and seven from hippocampus in each region, with three mice in each group, were analyzed. Cortical

and hippocampal total levels (*a*, *c*) and hippocampal typical regions' (CA1, CA3, DG) levels (*b*, *d*) are showed on the graph. **D** Western blotting of tTG in 3M, 6M, 9M, and 12M APP/PS1 and WT mice (n=6 for each group). Images were detected on Bio Imaging System (DNR Lumi BIS) via ECL system and analyzed by Image-Pro Plus 6.0. The figure is the representative bands of tTG and β-actin Western blotting. Statistical data is expressed as mean±SEM from independent experiments group. *P<0.05, **P<0.01, ***P<0.001 vs. 3 M groups or WT controls. #P<0.05, ##P<0.01, ###P<0.001 vs. WT controls

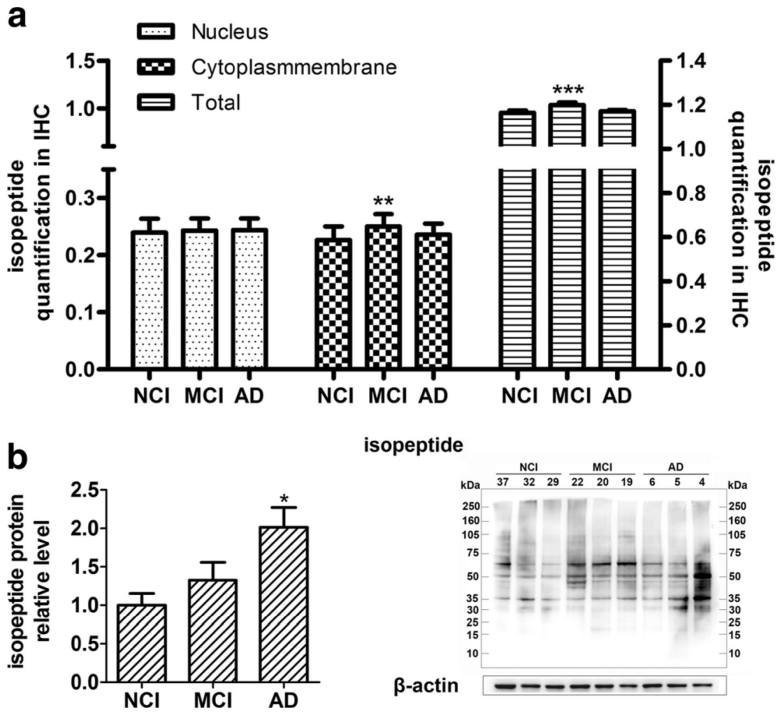

Fig. 4.

Alterations of isopeptide protein level in NCI, MCI, and AD. **a** Quantification of isopeptide immunohistochemical staining in NCI, MCI, and AD. Four sections with five samples in each group were analyzed. Resolution spectra images were quantitatively analyzed using art imaging systems Vectra™ (Caliper Life Sciences, Inc, Hopkinton, MA). Average positive OD values from roughly 150–300 cells were summarized. **b** Western blotting of isopeptide in NCI, MCI, and AD. Images were detect on Bio Imaging System (DNR Lumi BIS) via ECL system and analyzed by Image-Pro Plus 6.0 (n=10 for each group). Statistical data is expressed as mean±SEM from independent experiments group. *P<0.05, **P<0.01, ***P<0.001 vs. NCI group

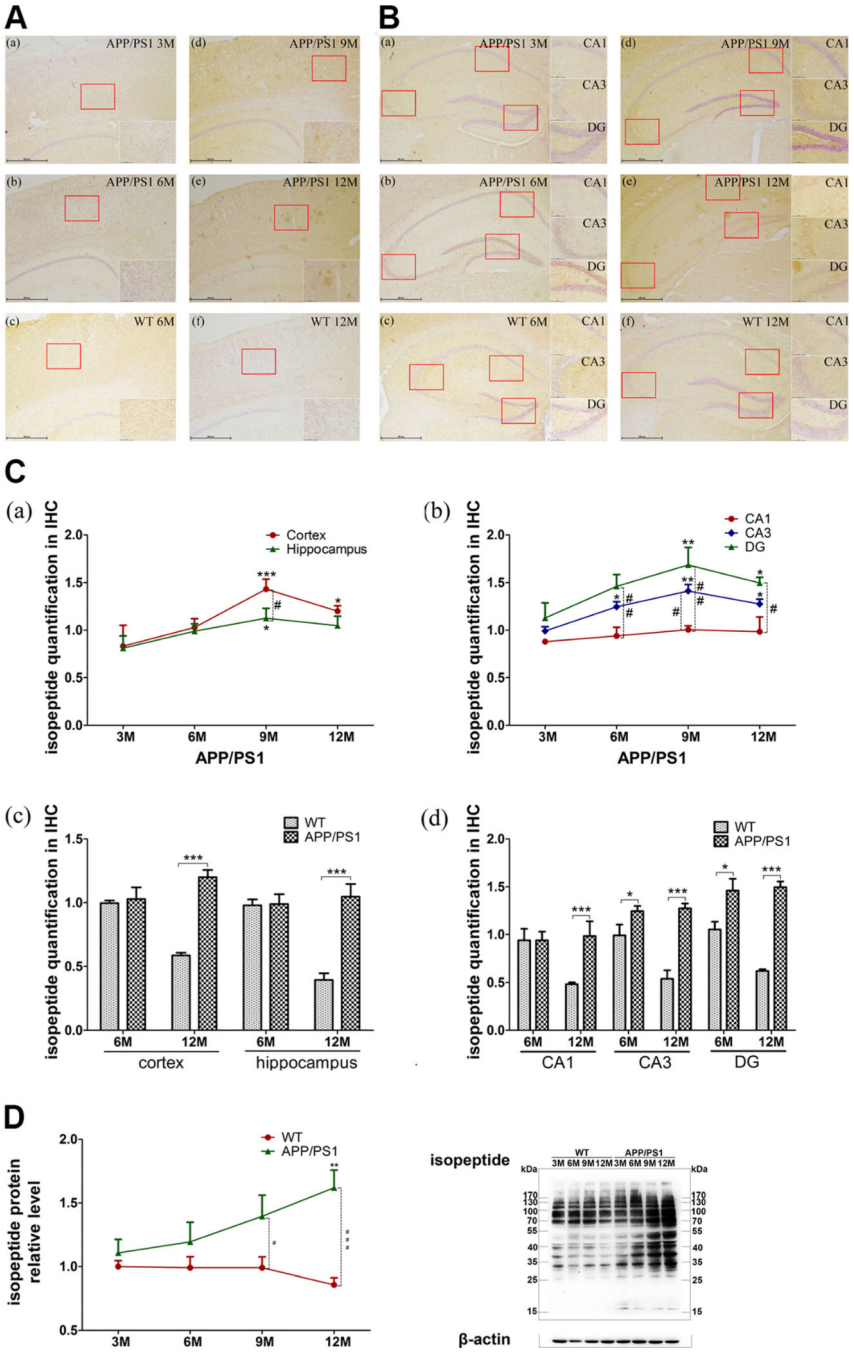

Fig. 5.

Protein cross-linking level in APP/PS1 and WT mice. **A, B** Immunohistochemistry of isopeptide in 3M (*a*), 6M (*b*), 9M (*d*), and 12M (*e*) APP/PS1 transgenic mice or 6M (*c*) and 12M (*f*) WT mouse cortex (**A**) and hippocampus (**B**). Imaging was captured in the bright-field mode via Nikon microscope with imaging system. The figure is the representative images with ×40 and ×200 magnification of IHC. **C** Data acquisition from isopeptide slices. The average signal intensity (IOD/AOI) of isopeptide in the cortex and hippocampus was calculated by using Image-Pro Plus 6.0 software. Six sections from cortex and seven from

hippocampus in each region, with three mice in each group, were analyzed. The total levels of cortex and hippocampus (*a*, *c*) and the levels of hippocampal subregions (CA1, CA3, DG) (*b*, *d*) are shown. **D** Western blotting of isopeptide in 3-, 6-, 9-, and 12-month WT and APP/PS1 mice. Images were detect on Bio Imaging System (DNR) via ECL system and analyzed by Image-Pro Plus 6.0 (n=6 for each group). The figure is the representative bands of isopeptide and β-actin Western blotting. Statistical data is expressed as mean ±SEM from independent experiment groups. *P<0.05, **P<0.01, ***P<0.001 vs. 3M groups or WT controls. #P<0.05, ##P<0.01, ###P<0.001 vs. WT controls

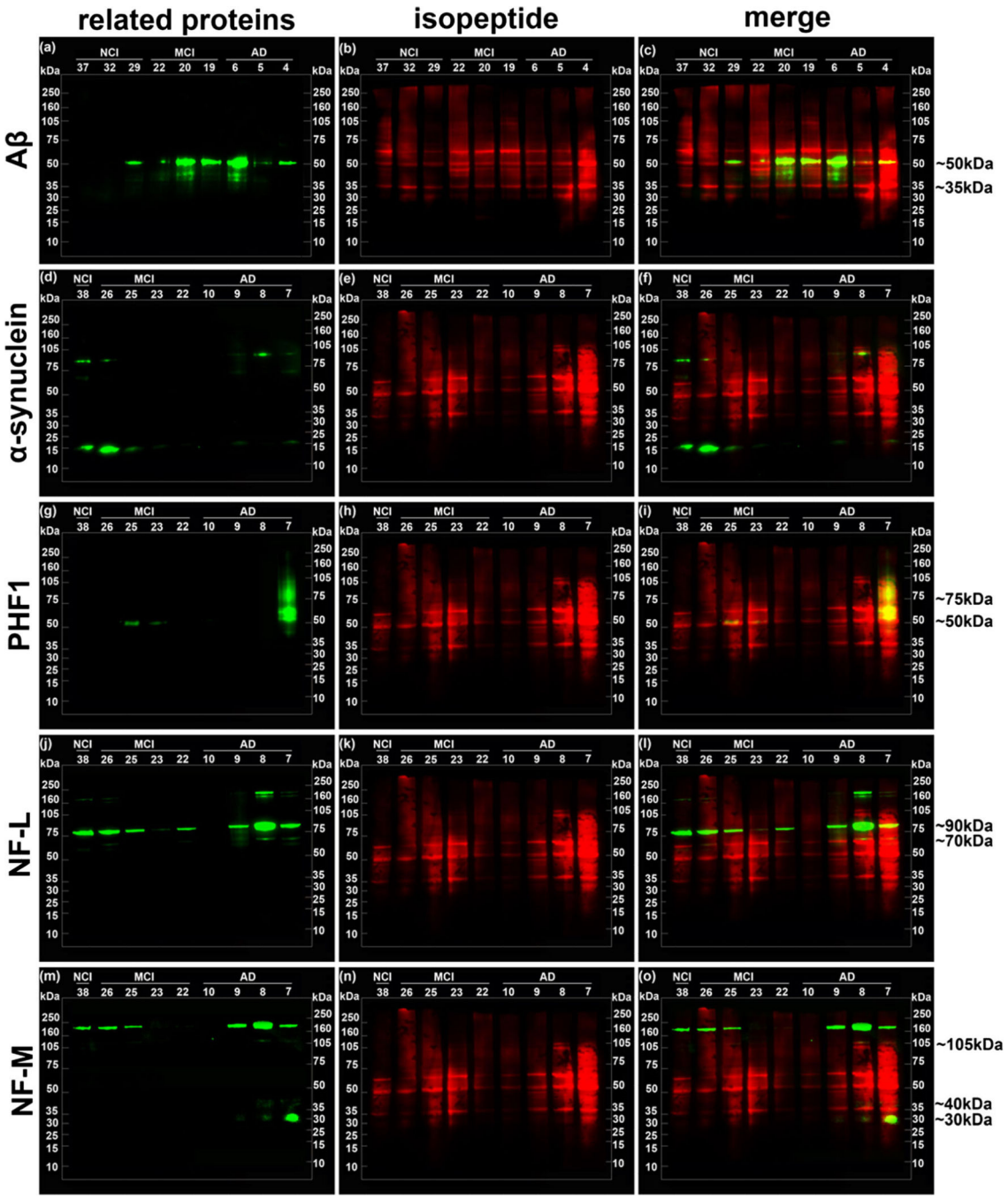

Fig. 6.

Isopeptide overlapping with relative protein in NCI, MCI, and AD brains. Overlapping of isopeptide and related proteins by immunoblotting detection. Pseudo-color technology was applied to show overlaps of Western bands. Isopeptide (*red*) and each related proteins (*green*) were detected on the same membrane. The bands of Aβ (*a*), α-synuclein (*d*), PHF1 (*g*), NF-L (*j*), and NF-M (*m*) were merged with isopeptide bands (*b*, *e*, *h*, *k*, *n*) to show overlap (*yellow*) (*c*, *f*, *i*, *l*, *o*), respectively. The figure is the representative bands to show. *Right line* represents approximate molecular weight of main overlaps

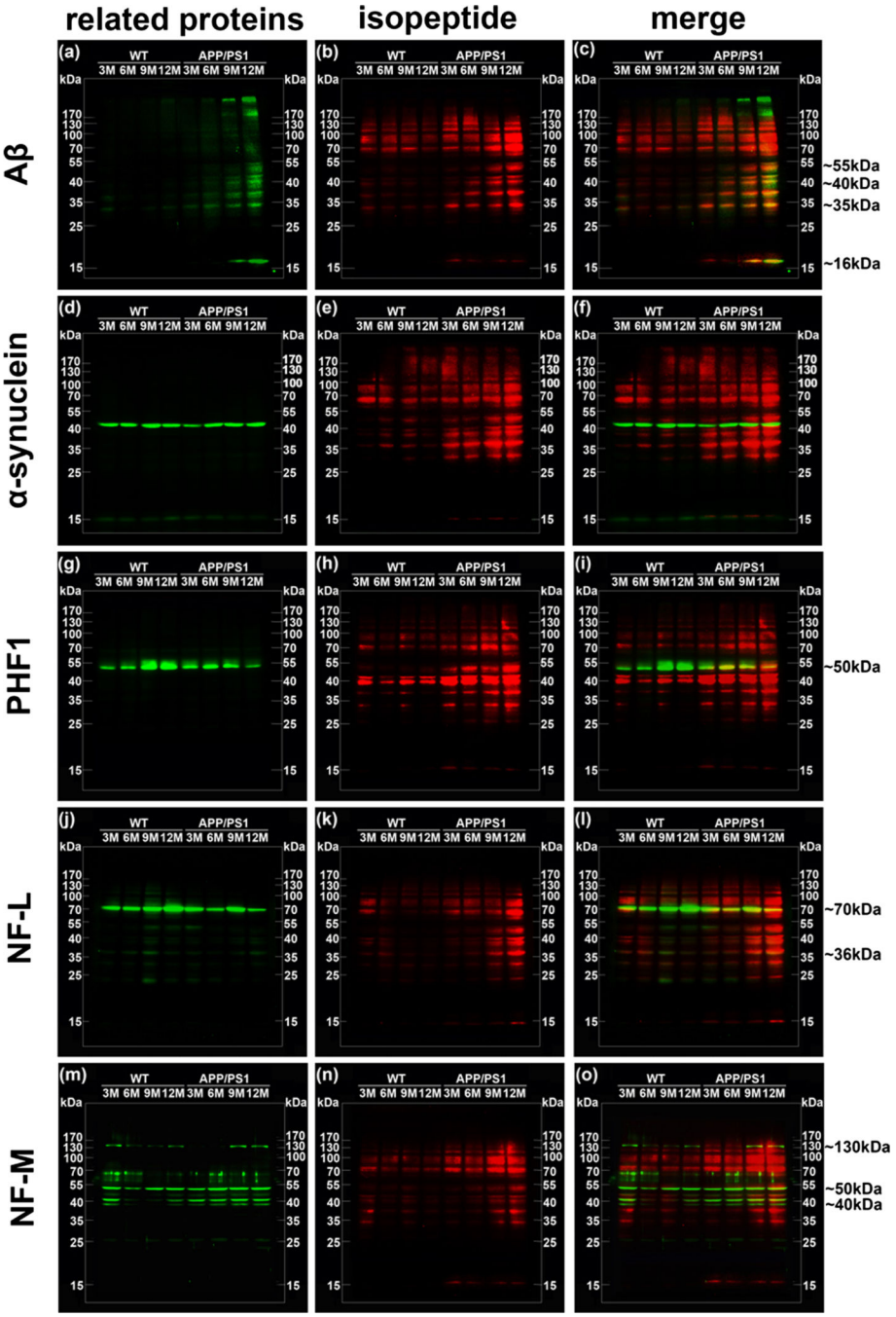

Fig. 7.

Isopeptide overlapping with relative protein in APP/PS1 and WT mice brains. Overlapping of isopeptide and related proteins by immunoblotting detection. Pseudo-color technology was applied to show overlaps of different protein bands. Isopeptide (*red*) and each related proteins (*green*) were detected on the same membrane. The bands of Aβ (*a*), α-synuclein (*d*), PHF1 (*g*), NF-L (*j*), and NF-M (*m*) were merged with isopeptide bands (*b*, *e*, *h*, *k*, *n*) to

show overlaps (*yellow*) (*c*, *f*, *i*, *l*, *o*), respectively. The figure is the representative bands to show. *Right line* represents approximate molecular weight of main overlaps